Modeling Energy Dissipation in a Tumbling Defunct Satellite using a Finite Element Method

Ryotaro Sakamoto and Daniel J. Scheeres
University of Colorado Boulder
429 UCB, Boulder, CO 80309

ABSTRACT

A detailed finite element model that captures energy dissipation effects on a tumbling satellite is presented. This model is used to estimate the relaxation time of a satellite in a complex rotation mode, enabling comparison with objects that have been observed to undergo rotational relaxation. This model can be used to develop better models for energy dissipation in non-uniformly rotating debris and defunct satellites.

1. INTRODUCTION

The transition of defunct satellite rotation states from uniform rotation to tumbling has been predicted and observed recently in the GOES-8 satellite [1]. These transitions are driven by solar radiation pressure torques, similar to the so-called "YORP Effect" which has been implicated in the evolution of asteroid rotation states [2]. The cycle observed for GOES-8 apparently involves periods of spin-up about the minimum axis of inertia followed by a period of energy dissipation, which brings the satellite back to rotation about its maximum moment of inertia. These dynamics raise a number of interesting question about the evolution of spinning defunct satellites and debris in general. In this research, we study one aspect of this cycle, focusing on the dissipation of energy. We develop detailed models for energy dissipation in flexible satellites, using finite element calculations to model the flexible dynamics of a satellite appendage subject to time-varying accelerations arising from a tumbling body. We use these calculations to model the energy dissipation in a satellite appendage over every periodic cycle. The simulations explore the amount of dissipation as a function of model parameters and as a function of the appendage orientation relative to the satellites principal axes. Using the resulting dissipation and model parameters for the satellite, we feed back the energy dissipation into the assumed torque-free rotation of the body to characterize the relaxation time scale. The goal of this research is to develop models that will enable the estimation of energy dissipation on observed satellites.

Our simulations model a simple solar array panel using a finite element method. Our models are two and three dimensional. To evaluate the response of the model to a tumbling satellite, we model a time-periodic acceleration profile distributed across the component, which has an additional offset from the ideal satellite center of mass. The acceleration acting at a specific point on the appendage is found by combining a torque-free angular rate and acceleration with the relative location of the component, and the finite element method computes the distributed dynamical effect of these accelerations across the appendage. As the accelerations are periodic in the body-fixed frame, the simulations are run over a long enough time for the behavior to settle into a steady oscillation. As the local level of dissipation is increased, the amplitude of the oscillations become smaller. To determine the overall effect on the body spin rate it is necessary to determine the total energy transferred into the appendage oscillation in the absence of dissipation, comparing the peak energy to the dissipation over each cycle. To measure this empirically we track the total amplitude of the steady-state oscillations as the dissipation in the appendage is decreased. The following work demonstrate the results of the amount of the energy dissipation numerically. Each result is considered with various spin rate and dumping coefficient. Numerical analyses are conducted as two and three dimensional respectively. The method of the setting up these models are introduced briefly at the beginning of the section. This allows the parameter Q to be computed, which can then be directly used to compute the energy dissipation rate. This can be used to modify the spin state in a predictable way, allowing for the relaxation of the excited spin state to be tracked over longer time spans, and evaluated at varying levels of excitation. These calculations will be compared with observations of the tumbling satellite GOES-8 [1] to develop empirical estimates of what appropriate level of dissipation should be used in our simulations for this particular asteroid.

2. STRUCTUAL MODEL

In this section, we discuss the Finite Element Method and the analysis models applied in this research. FEM is used as a tool to evaluate the material properties and their dissipation effectively [3]. As shown in Fig. 1 each element has two nodes. L indicates the length of an element. Additionally, node coordinate matrices are also defined as in Eq. (1) and (2). For two-dimensional analysis, the node coordinate has three components, X, Y, and the angle between them. For three-dimensional analysis, the Z direction is added to X and Y and the resulting degrees of freedom are 6, X, Y, Z, and the angles between them. The circled number in Fig. 1, indicates the node number.

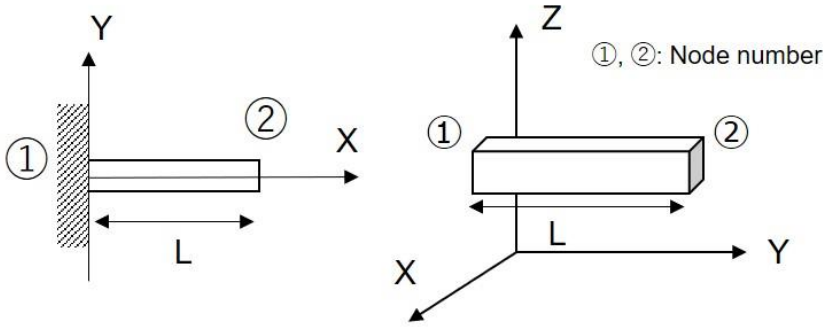

Fig. 1. Elements and nodes number (Left: 2D, Right: 3D)

$$\textbf{Node Coordinate (2D)} = (\boldsymbol{X} \quad \boldsymbol{Y} \quad \boldsymbol{Z}), \textbf{Node Matrix (2D)} = \begin{pmatrix} \boldsymbol{Node①} \\ \boldsymbol{Node②} \end{pmatrix} = \begin{pmatrix} \mathbf{0} & \mathbf{0} & \mathbf{0} \\ \mathbf{1} & \mathbf{0} & \mathbf{0} \end{pmatrix} \tag{1}$$

$$\textbf{Node Coordinate (3D)} = (\boldsymbol{X} \quad \boldsymbol{Y} \quad \boldsymbol{Z}),$$
$$\textbf{Node Matrix (3D)} = \begin{pmatrix} \boldsymbol{Node①} \\ \boldsymbol{Node②} \end{pmatrix} = \begin{pmatrix} \mathbf{1} & \mathbf{0} & \mathbf{1} \\ \mathbf{1} & \mathbf{1} & \mathbf{1} \end{pmatrix} \tag{2}$$

Based on these fundamentals, we developed analysis models as shown in Fig. 2. The left model is for two-dimensional analysis, the right one is for three-dimensional analysis with X Y Z axes. These setups are simulated for a typical satellite model. cubes of each model indicate the main body component of satellites. The rightmost plates model solar array panels. Each model has a total of seven or twenty-nine elements, respectively. In this research, the material properties were set as aluminum, with parameters as shown in Tab. 1 [4]. As shown in this table, the Length of one element is set at 1.0 [m]. Therefore, total size of two-dimensional model is with 4.0 m (X direction) × 2.0 m (Y direction). The three-dimensional models has 1.0 m (X direction) × 4.0 m (Y direction) × 2.0 m (Z direction). Parameters of the transverse module are only applied for the three-dimensional analysis.

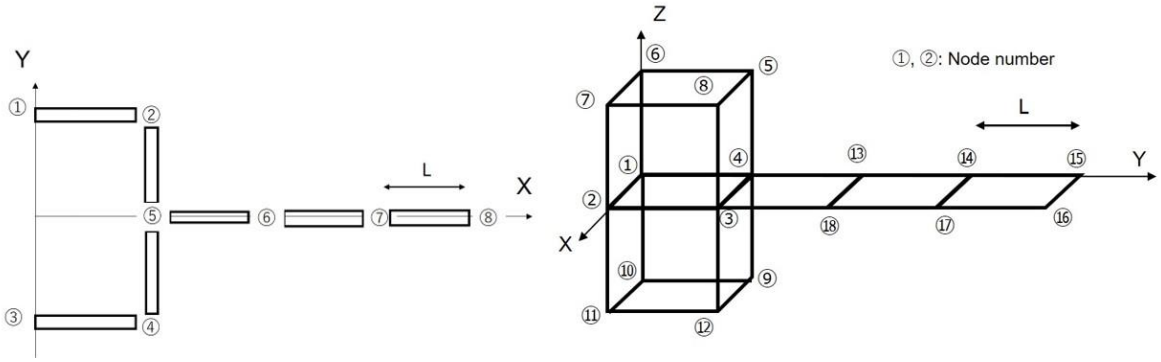

Fig. 2. Analysis model (Left: 2D, Right: 3D)

Tab. 1 Parameters of structural model

Parameter	Value
Length of an element: L [m]	1.0
Thickness [m]	0.002
Width [m]	0.02
Density [kg/m^3]	2857.4
Modulus of elasticity [GPa]	70.0
Transverse modulus of elasticity [GPa]	28.0

3. NUMERICAL ANALYSIS

3.1 Dynamical Equation

In this analysis, in order to investigate various system responses, damping was included in the simulations [5]. Here, M is the mass matrix, C is the damping coefficient, K is the stiffness matrix, and X is state. This equation is a second order differential equation and therefore was modified into a first order equation with $X = x_1$, $\dot{X} = x_2$, as shown as Eq. (4)

$$\boldsymbol{M\ddot{X} + C\dot{X} + KX = F} \tag{3}$$

$$\begin{pmatrix} \dot{x_1} \\ \dot{x_2} \end{pmatrix} = \begin{pmatrix} \mathbf{0} & 1 \\ -\frac{K}{M} & -\frac{C}{M} \end{pmatrix} \begin{pmatrix} x_1 \\ x_2 \end{pmatrix} + \begin{pmatrix} 0 \\ \frac{1}{M} \end{pmatrix} F \tag{4}$$

For the two-dimensional FEM analysis, each X state and F matrix are defined as following. The X state has difference information for x, y direction, and angle. The F matrix is described by the force along the x and y direction.

$$X - state = \begin{pmatrix} Displaecment(x) \\ Displacement(y) \\ Angle \end{pmatrix}, F = \begin{pmatrix} x \\ y \\ Moment \end{pmatrix} \tag{5}$$

3.2 Rotational Acceleration Matrix

To model a satellite tumbling motion, we add rotational acceleration matrix as a time-varying acceleration. The following equations present the two and three dimensional acceleration matrices. Here $\omega_\perp$ represents a perpendicular vector relative to the rotational axis.
For two-dimensional analysis,

$$a = \begin{pmatrix} \omega^2 r - \omega_\perp^2 r cos^2(\omega_0 t) \\ -r \times \omega_\perp^2 \sin(\omega_0 t)\cos(\omega_0 t) \\ 0 \end{pmatrix} \tag{6}$$

Where, $\omega_0 = \frac{2\pi}{3600}, \omega_\perp = \alpha \times \omega_0, \omega^2 = \omega_0^2 + \omega_\perp^2$

For three-dimensional analysis, the r vector is given by node coordinate matrices in section 2.

$$a = \begin{pmatrix} \omega^2 - \omega_\perp^2 cos^2(\omega_0 t) & -\omega_\perp^2 sin(\omega_0 t)cos(\omega_0 t) & -\omega_\perp \omega_0 cos(\omega_0 t) \\ -\omega_\perp^2 \sin(\omega_0 t)\cos(\omega_0 t) & \omega^2 - \omega_\perp^2 sin^2(\omega_0 t) & -\omega_\perp \omega_0 sin(\omega_0 t) \\ -\omega_\perp \omega_0 cos(\omega_0 t) & -\omega_\perp \omega_0 sin(\omega_0 t) & \omega^2 - \omega_0^2 \end{pmatrix} \vec{r} \quad (7)$$

Where, $\vec{r} = \begin{pmatrix} x \\ y \\ z \end{pmatrix}$

Fig. 3 shows the exaggerated motion as the models are rotating. Left figure is shown when the two-dimensional model is oscillating about the Y axis. Node 1 and 2 are considered as fixed. On the right is the three-dimensional model oscillating about the X axis. As with the two-dimensional analysis, the origin of the model, node 1, is fixed.

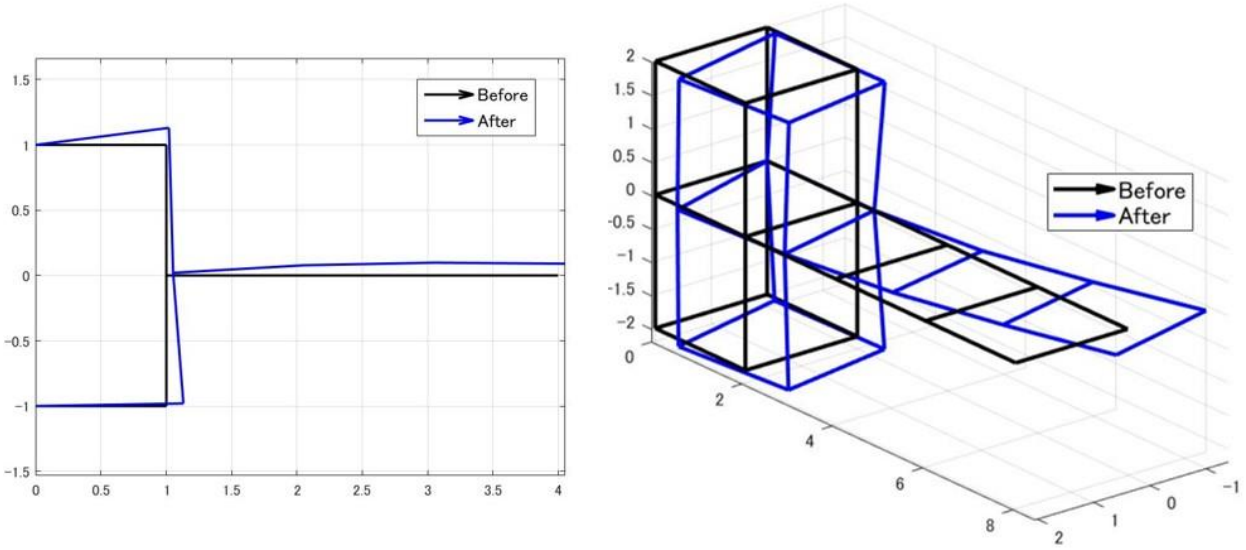

Fig. 3. The images of the behaviors as model rotation (Left: 2D, Right: 3D)

4. SIMULATION RESULTS

4.1 Parameters and Overview

This section presents results of the calculations. Using these methods, as discussed above, we compute the energy dissipation in several situations. We mainly change the rotational rate (ω_0) and damping coefficient (C) as free parameters. Generally, attenuation of a system is caused by friction between the components of structure and sloshing of liquid inside the system [6]. Also, structural attenuation is often discussed. However, in this study, we did not focus on the factor of the attenuation. That is, we parametrize damping coefficient as a general attenuation. For two-dimensional analysis, Eq (6) was taken into numerical simulation directly. Then, results are shown with the models' position difference, velocity, potential energy, and kinetic energy. These energies are calculated based on following equations.

$$\boldsymbol{Potential\ enrgy} = \frac{\mathbf{1}}{\mathbf{2}} \boldsymbol{X^t K X}$$
$$\boldsymbol{Kinetic\ enrgy} = \frac{\mathbf{1}}{\mathbf{2}} \boldsymbol{\dot{X}^t M \dot{X}} \quad (8)$$

4.2 Two-Dimensional analysis

Calculation results in two-dimension are shown in this section. Fig. 4 indicates the time history of the tip position (Node 8 at Fig. 2 left) and velocities. Right side of Fig. 4 focuses on potential energy and kinetic energy. Each colored line represents a damping coefficient ranging from 0.05 to 1. The rotational rate was set as $2\pi/300$ [deg/sec]. We confirmed that the peak of each amplitude is decaying as damping gets larger. For two energies figure, the difference of the peak of each amplitude, which means the amount of energy dissipation, depends on damping coefficient. For instance, the purple line indicates the maximum energy with the damping coefficient is at a minimum value. In contrast, the blue line's amplitude with damping coefficient equal to one, is lower than purple's. Fig. 5 shows the tendency of the total energy dissipation with damping coefficient. Total energy is summed up potential and kinetic energies. Plots were from the values each coefficient values. We confirmed two characteristics about rate of energies dissipation. One is from the left side another is the right side in Fig. 5. The rate of energy dissipation is coincidence even as the rotational rates are different. Second thing is that the rate of energy dissipation is decreasing dramatically, as rotational speed gets faster.

To reach the concrete results, we plotted potential energy along horizontal axis versus positional difference of the tip position at node 8 along on the vertical axis in Fig. 6. Rotational rate was set as $2\pi/600$. From left up to right bottom, the damping coefficient gets larger. Like hysteresis analysis, we calculated the area of each curve. Each figure in Fig. 6 is one oscillation period respect to damping coefficient. The area help us understand the energy dissipation as one cycle oscillation. Calculation results of area are shown in Fig. 7 rotational rates are $2\pi/600$, $2\pi/1800$, $2\pi/3600$ respectively. From Fig. 6 and 7, we also confirmed the two tendency we mentioned above.

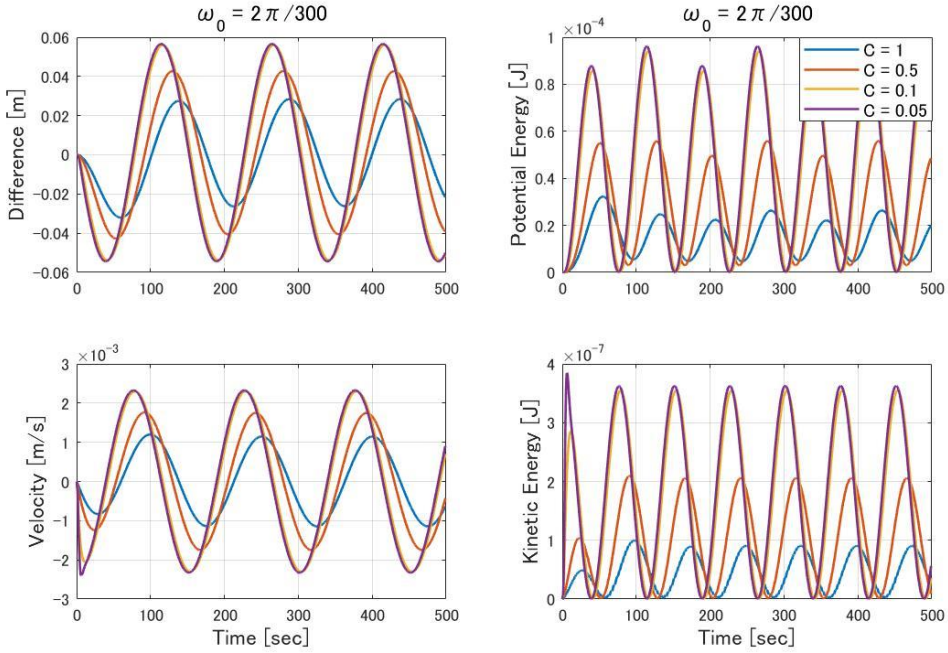

Fig. 4. Time history of the tip position (node 8) and energies

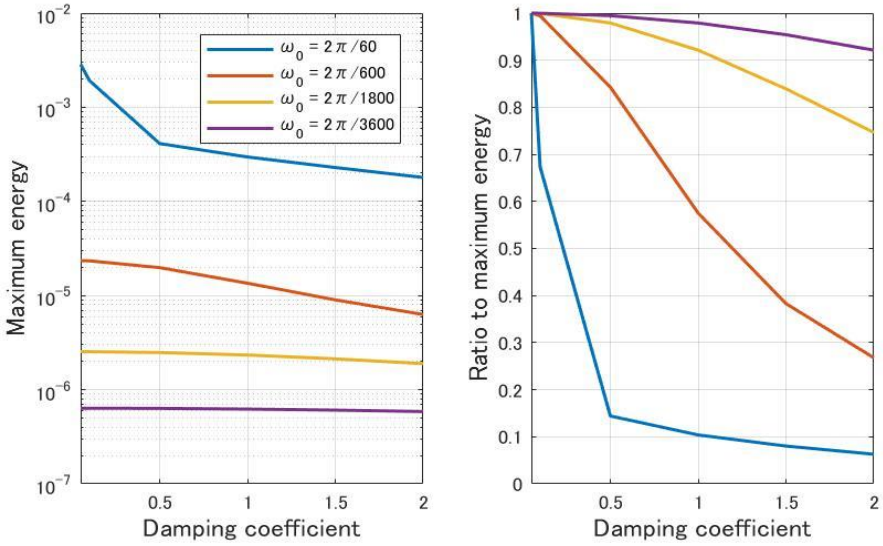

Fig. 5. The rate of the energy dissipation with respect to the damping coefficient (2D)

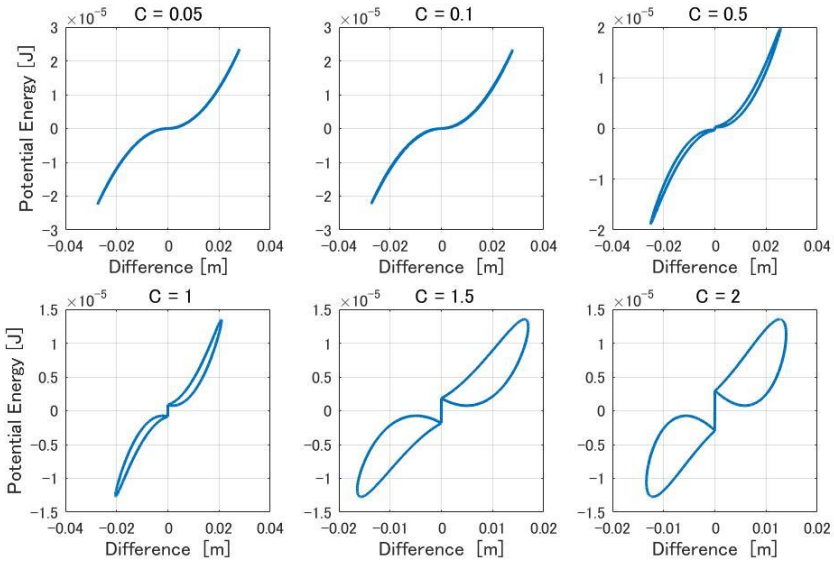

Fig. 6. Area of Potential energy (ω = 2π/600)

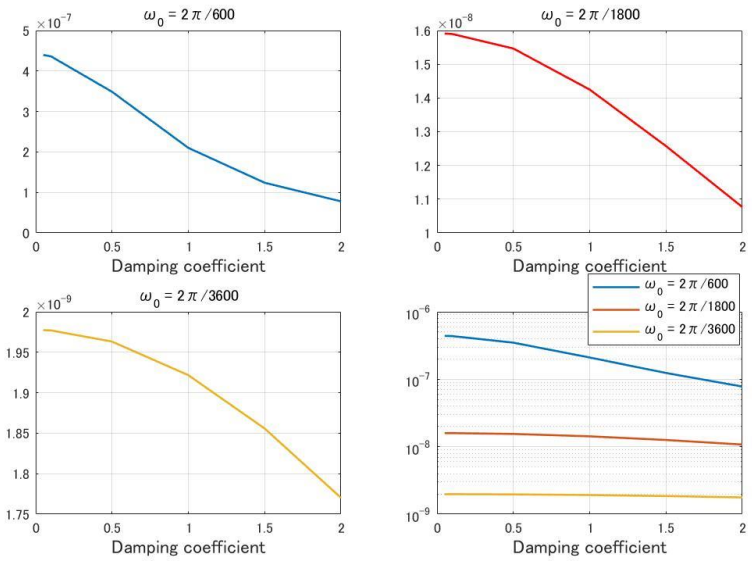

Fig. 7. Area of potential energy respect to damping coefficient (2D)

4.3 Three-Dimensional Analysis

Similar to section 4.2, we also demonstrate the result of our three-dimensional calculations and confirm the tendency between rotational rate and the amount of the energy dissipation. For three-dimensional analysis, we take X axis rotation based on Eq. (7) to get reasonable results. We also could reach two tendencies in three-dimensional analysis same as the as the two-dimensional ones. The first thing is that the amount of the energy dissipation gets larger as the damping coefficient gets larger. The left side of Fig. 8 shows the position difference at the tip of the model, which is node at 15 of the right side of Fig. 2. From up to bottom figure is showing X, Y, and Z axis respectively. The right side of Fig. 8 is the time history of the potential and kinetic energies. Each colored line stands for the damping coefficient. Rotational rate is set as $2\pi/300$. Like two-dimensional analysis, we confirmed the energy dissipation depends on the damping coefficient. The peaks of each oscillation get smaller as the damping coefficient get larger. The amount of difference of the peak means the amount of energy dissipation we estimated.
The second thing is that the rate of the energy dissipation is faster as the rotational rate gets faster. Fig. 10Fig. 9 shows more detailed results, which have rotational rates from $2\pi/60$ to $2\pi/1200$. On the left side of Fig. 10, we plotted the positioning difference along the X axis of the model and potential energy. Damping coefficient is also compared in this figure. The right side of Fig. 10 shows the time history of the three-dimensional difference at node 15.

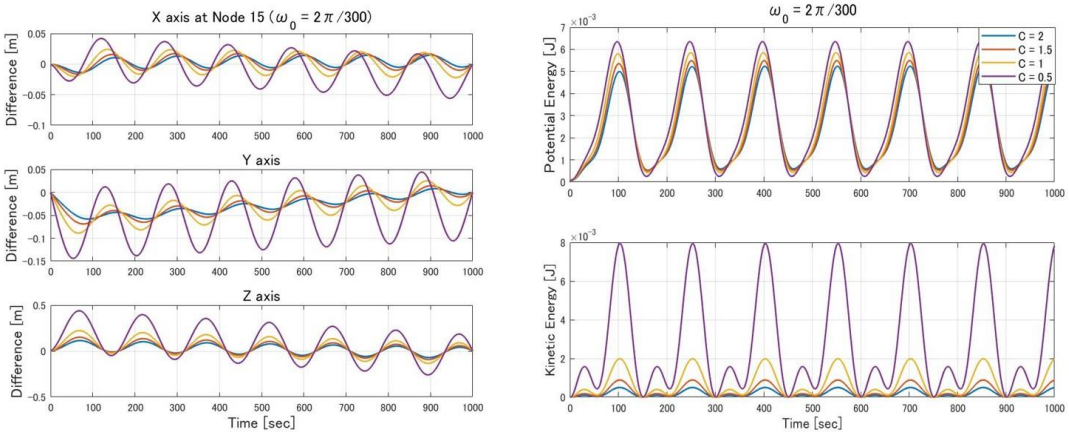

Fig. 8. Time history of the tip position (node 15) and energies

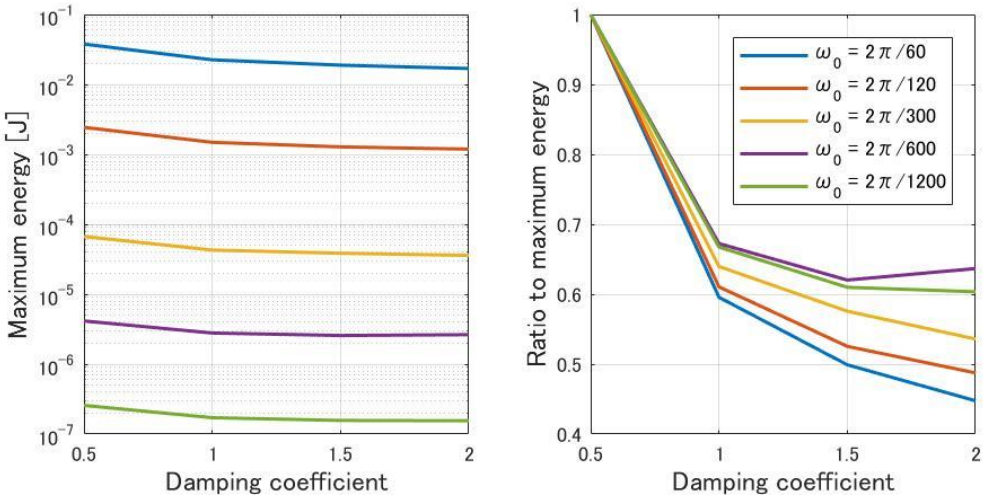

Fig. 9. The rate of the energy dissipation with respect to damping coefficient (3D)

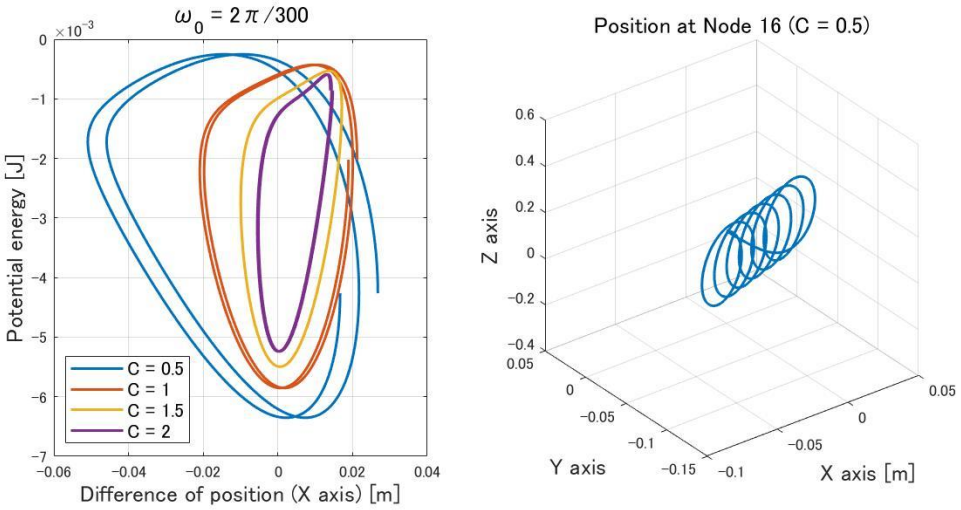

Fig. 10. Area of potential energy (Left) and position histry at node 16 (Right) ($\omega_0 = 2\pi/300$)

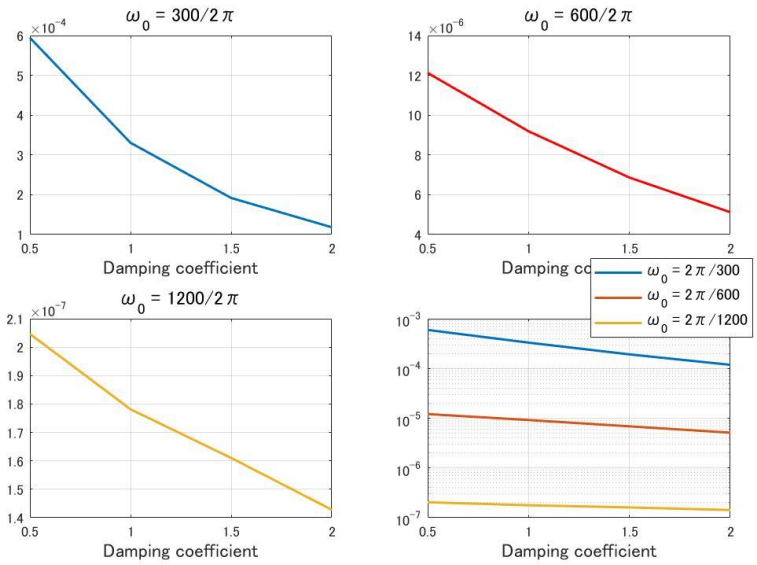

Fig. 11. Area of potential energy respect to damping coefficient (3D)

5. CONCLUSION

In order to calculate the energy dissipation rate in a tumbling satellite we quantitatively investigated the relationship between energy dissipation, rotation rate, and damping coefficient, we established simple satellite models with FEM. We computed the energy dissipation with two and three-dimension models. Several results were shown in above section. The decay of the amplitude of the energies, considering the depend on the rotation rate and the damping coefficient, were revealed. Additionally, numerical simulations for two and three dimensional demonstrated the similar tendency for dissipating energy. We believe these results would contribute the way of modifications the rotation rate or axis to stabilize the detumbling satellites or asteroids. However, these analyses only offer simple axis rotation. To truly understand and predict the rotation state and the energy dissipation, more complicated rotational acceleration modeling is needed. The next steps in this research will expand these models and consider the effect of feeding back the computed level of dissipation into the evolving simulations.

6. REFERENCES

1. A. Albuja, D.J. Scheeres, R.L. Cognion, W. Ryan and E.V. Ryan. 2018. “The YORP Effect on the GOES 8 and GOES 10 Satellites: A Case Study,” *Advances in Space Research 61*: 122-144.
2. D.P. Rubincam. 2000. “Radiative spin-up and spin-down of small asteroids,” Icarus 148(1): 2-11.
3. Komatsu, K., *Mechanical structure vibration engineering*, Morikita Publishing Co., Ltd, Tokyo, Japan, 2012. (in Japanese)
4. Sakamoto, R., Tanaka, H. and Ogi, Y., “Improvement of deployment repeatability by the vibration produced by macro fiber composite actuator”, *Bulletin of the JSME Mechanical Engineering Letters, Vol.2. No. 16-00042, 2016*, pp.1-8.
5. Kojima, Y., Taniwaki, S., and Okami, Y., “Dynamic simulation of stick-slip motion of a flexible solar array”, *Control Engineering Practice, Vol. 16, 2008*, pp. 724-735.
6. Tsuboi, M., “Report of the circumstances and the discontinuation of Astro -G project”, Japan VLBI Consortium, Tokyo, Japan, 2011. (in Japanese).